Dimerization of Tie2 mediated by its membrane-proximal FNIII domains

Jason O. Moore[a,b], Mark A. Lemmon[a,1,2], and Kathryn M. Ferguson[b,1,2]

[a]Department of Biochemistry and Biophysics, University of Pennsylvania Perelman School of Medicine, Philadelphia, PA 19104; and [b]Department of Physiology, University of Pennsylvania Perelman School of Medicine, Philadelphia, PA 19104

Edited by Tony Hunter, The Salk Institute for Biological Studies, La Jolla, CA, and approved March 23, 2017 (received for review October 26, 2016)

Tie1 and Tie2, members of the tyrosine kinase family with immunoglobulin and EGF homology domains, are receptor tyrosine kinases found primarily in endothelial cells with key roles in development and maintenance of the vasculature and in angiogenesis. They are attractive targets for therapeutic intervention in tumor angiogenesis, inflammation, and sepsis. Tie2 is regulated directly by the multimeric angiopoietin (Ang) ligands, with Ang1 being its primary activator. Structural studies have shown how Angs bind to the Tie2 ligand-binding region, but do not explain Tie2 activation and suggest a passive role for the Tie2 extracellular region (ECR) in ligand-induced receptor dimerization. Here we show that the Tie2 ECR forms strong dimers even in the absence of bound ligand. Dimerization is mediated by membrane-proximal fibronectin type III (FNIII) domains that were omitted in previous structural studies. We describe a 2.5-Å resolution X-ray crystal structure of the membrane-proximal three Tie2 FNIII domains, Tie2(FNIIIa–c), revealing two possible dimerization modes that primarily involve the third FNIII domain, FNIIIc. Mutating these dimer interfaces implicates one of them (dimer 1) in soluble Tie2 (sTie2) dimerization in solution but suggests that both could play a role in Ang1-induced Tie2 activation, possibly modulated by Tie1. Through small-angle X-ray scattering studies of sTie2 dimers in solution and modeling based on crystal structures, we suggest that Ang1 binding may cross-link Tie2 dimers into higher-order oligomers, potentially explaining how Tie2 is differentially clustered following ligand engagement in different cellular contexts. Our results also firmly implicate FNIII domain-mediated interactions in Tie2 activation, identifying a potential Achilles' heel for therapeutic inhibition.

receptor tyrosine kinase | dimerization | angiopoietin | Tie | crystallography

The Tie family [named as "**t**yrosine kinases with **i**mmunoglobulin and **E**GF homology domains" (1)] of receptor tyrosine kinases (RTKs) contains two members, Tie1 and Tie2/TEK, that are expressed primarily on endothelial cells and control cellular responses to the angiopoietin (Ang) ligands (2, 3). Tie1 and Tie2 play important roles in the development of normal vasculature, in vascular homeostasis, and in angiogenesis (4, 5). Tie receptor signaling therefore has emerged as an attractive target for therapeutic intervention in tumor angiogenesis, inflammation, and sepsis (6, 7). Regulation of Tie receptors is complex and poorly understood. Tie2 binds all the Ang ligands (Ang1, Ang2, and Ang4 in humans) but with quite different signaling consequences (2, 8–11). The closely related Tie1, by contrast, does not bind directly to any of the Angs, although it clearly pays a crucial role as a coreceptor and modulates Tie2 signaling and cellular responses to the different Angs (12). Focusing on Tie2, receptor activation and autophosphorylation can be promoted directly by multimeric Ang1 and appears to involve ligand-induced oligomerization, as seen with other RTKs (13). Ang1 dimers can activate Tie2 expressed ectopically in model cell systems (14), but higher-order Ang1 multimers are needed to activate Tie2 in its native endothelial cell context (14), probably reflecting the involvement of Tie1 in Tie2 regulation (12, 15). Similarly, although Ang2 can activate Tie2 expressed in NIH 3T3 cells, this ligand instead functions as an antagonist or partial agonist in endothelial cells and in vivo (9, 16, 17). The cellular context also dramatically alters the signaling consequences of Tie2 activation. Whereas Tie2 activation in mature vessels promotes maintenance of vascular integrity and endothelial cell survival, it instead promotes endothelial cell proliferation and migration during angiogenesis (4). These stark signaling differences appear to arise, at least in part, from the altered subcellular location of Tie2 and/or from differences in Tie2 (or Tie1/Tie2) clustering or oligomerization following engagement by Angs in different cellular contexts (18, 19).

Each Ang has a C-terminal receptor-binding fibrinogen-related domain (FReD) linked through a coiled-coil region to a functionally crucial Ang clustering domain (14). The Ang FReDs bind to a membrane-distal ligand-binding region (LBR) of Tie2 that contains three Ig-like domains plus three EGF domains (20, 21). Ang binding does not induce conformational alterations in the Tie2 LBR, indicating that Tie2 oligomerization and signaling are most likely specified by Ang multimerization (14) and/or by Tie1 interactions (12, 15, 16), with the Tie2 extracellular region (ECR) playing a passive role. C-terminal to the Tie2 LBR, however, are three membrane-proximal fibronectin type III (FNIII) domains (Fig. 1*A*) that have not been well studied. By analogy with

Significance

Tie2 is a receptor tyrosine kinase with important roles in vascular development. Inhibiting Tie2 may impair tumor angiogenesis, whereas activating Tie2 may be beneficial in sepsis and inflammation. To modulate Tie2 therapeutically, it is essential to understand its regulation. Although it is known how Tie2 binds its activating ligands (angiopoietins), it is not clear how this binding (or Tie1 interactions) regulates the receptor. Here, we show that the previously unstudied Tie2 extracellular membrane-proximal region engages in receptor–receptor contacts crucial for Tie2 activation. Our data suggest that angiopoietins promote receptor clustering, utilizing Tie2–Tie2 interactions mediated by key fibronectin III domains, a unique mode of RTK activation. Blocking these Tie2–Tie2 interactions may have therapeutic value in cancer.

Author contributions: J.O.M., M.A.L., and K.M.F. designed research; J.O.M. and K.M.F. performed research; J.O.M., M.A.L., and K.M.F. analyzed data; and J.O.M., M.A.L., and K.M.F. wrote the paper.

The authors declare no conflict of interest.

This article is a PNAS Direct Submission.

Freely available online through the PNAS open access option.

Data deposition: Crystallography, atomic coordinates, and structure factors described in this paper have been deposited in the Protein Data Bank (PDB) database (PDB ID code 5UTK).

[1]Present address: Yale Cancer Biology Institute, West Haven, CT 06516, and Department of Pharmacology, Yale University School of Medicine, New Haven, CT 06520.

[2]To whom correspondence may be addressed. Email: mark.lemmon@yale.edu or kathryn.ferguson@yale.edu.

This article contains supporting information online at www.pnas.org/lookup/suppl/doi:10.1073/pnas.1617800114/-/DCSupplemental.

other RTKs (13, 22), we reasoned that these membrane-proximal FNIII domains, which were missing from previous Tie2 crystal structures, might self-associate and influence Tie2 signaling. Here we show that the extracellular FNIII domains of Tie2 do indeed self-associate. We map the interactions and observe two possible dimerization modes in a crystal structure of the membrane-proximal region. Mutations in one of the observed dimer interfaces, which includes a residue mutated in primary congenital glaucoma (23), disrupt both Ang1-induced Tie2 activation and dimerization of the Tie2 ECR in solution. Interestingly, mutations in the other interface also have some effect on Tie2 signaling, suggesting that both interfaces might play roles in clustering of the activated receptor. Visualizing these dimerization modes is important for understanding mechanisms of Tie receptor activation and clustering as well as the differential activation of Tie2 in distinct cellular contexts. Moreover, targeting these membrane-proximal interactions to inhibit Tie2 activity, as seen for other RTKs (24, 25), may have therapeutic value.

Results

The Tie2 ECR Forms an FNIII Domain-Mediated Dimer. To understand how clustered Angs can induce discrete Tie2 oligomerization, we undertook biophysical studies of the complete soluble ECR of the receptor (sTie2), secreted from baculovirus-infected Sf9 cells. Whereas previously studied Tie2 ECR fragments (without the FNIII domains) were monomers (21, 26), the complete sTie2 molecule sediments as a dimer in sedimentation equilibrium analytical ultracentrifugation (SE-AUC) studies (Fig. 1*B*). Even at 2 μM, sTie2 sediments (red circles in Fig. 1*B*) as would be predicted for a 163-kDa dimer (black line in Fig. 1*B*) rather than as a monomer (gray line in Fig. 1*B*). Global fitting of SE-AUC data to a monomer–dimer equilibrium suggested a K_d value of 1.63 ± 0.48 μM for sTie2 dimerization, strong enough to drive dimerization of at least half of the intact Tie2 in the membrane of a cell with 10,000 copies (27). By contrast, protein lacking all three FNIII domains failed to self-associate even at 10 μM (26), and protein lacking the two most C-terminal FNIII domains crystallized as a monomer (21). We generated an sTie2 ECR fragment lacking only the most C-terminal FNIII domain, sTie2(ΔFNIIIc), and found by SE-AUC that it sediments as a monomer (Fig. 1*C*), with a K_d > 1 mM. Thus, FNIIIc plays a key role in sTie2 dimerization, although we cannot exclude the possibility of contributions from other domains.

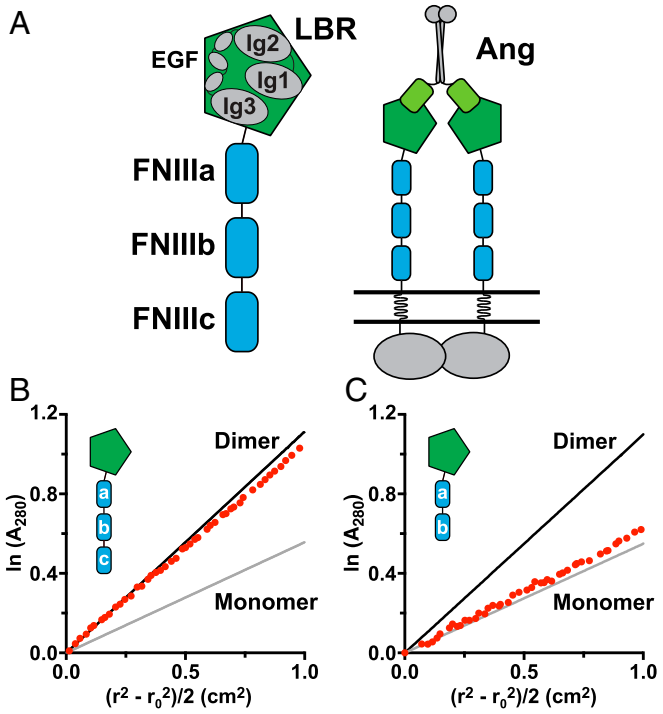

Fig. 1. The Tie2 ECR dimerizes via its membrane-proximal FNIII domain. (*A*) Cartoon of the hypothetical Ang-induced Tie2 dimer. The LBR, with three Ig and three EGF domains, is shown as a green pentagon. Binding of the FReDs (light green) promotes Tie2 oligomerization. Membrane-proximal FNIII domains are blue, and the cytoplasmic kinase domain of Tie2 (gray oval) is connected to the ECR by a single transmembrane helix. (*B* and *C*) SE-AUC data (red circles) for 2 μM sTie2 at 7,000 rpm (*B*) and 2 μM sTie2(ΔFNIIIc) at 7,500 rpm (*C*). Data are plotted as the natural logarithm of the normalized absorbance at 280 nm [$\ln(A_{280})$] as a function of the square of the radial distance (r) from the meniscus (r_0). For single species, this representation yields a straight line with slope proportional to molecular mass. Lines with predicted slopes for monomer [81.4 kDa for sTie2 and 70.6 kDa for sTie2(ΔFNIIIc)] and dimer [163 kDa for sTie2 and 141 kDa for sTie2(ΔFNIIIc)] are gray and black, respectively. The K_d from three biological replicates was 1.63 ± 0.48 μM.

Crystal Structure of the FNIII Domain Region of Tie2. We next used X-ray crystallography to visualize details of FNIII domain-mediated sTie2 dimerization. We could not grow suitable crystals of sTie2, but an *Escherichia coli*-expressed fragment containing all three membrane-proximal FNIII domains, Tie2(FNIIIa–c), yielded crystals diffracting to 2.5-Å resolution. We solved the structure using experimental phases determined by combining multiple isomorphous replacement (MIR) and multiwavelength anomalous dispersion (MAD) with the crystallographic parameters listed in Table S1. Tie2(FNIIIa–c) crystallized with two molecules in the asymmetric unit. The three FNIII domains were well resolved in experimental electron density maps (Fig. S1*A*), and the structure was refined to R_{work}/R_{free} of 22.5/24.7.

Each domain adopts a canonical FNIII domain fold; a sandwich of two antiparallel β-sheets comprising three and four β-strands, respectively (Fig. 2*A*), with topology A-B-E and G-F-C-C′ using C2-set Ig domain nomenclature. The three FNIII domains form an extended structure, with the direction of the long axis of FNIIIb deviating by 25–26° (tilt angle) from that of FNIIIa, and FNIIIc deviating by 60–66° from FNIIIb (Fig. 2*A*, Fig. S1*B*, and Table S2). The FNIIIb β-sandwich is rotated ∼180° about its long axis (twist angle) with respect to that of FNIIIa, so that the A-B-E sheet of FNIIIa lies on the same side of the structure as the G-F-C-C′ sheet of FNIIIb (Fig. 2*A*). The FNIIIc β-sandwich is twisted so that its sheets are almost orthogonal to those of FNIIIa and b. It also should be noted that, compared with the low-resolution structure of FNIIIa in Protein Data Bank (PDB) entry 4K0V (21), we see a shift in register by two residues, beginning around residue 486 in the loop between strands C and C′.

Structural Basis for FNIII Domain-Mediated Tie2 Association: Two Modes of Dimerization. Crystal packing suggests two possible Tie2(FNIIIa–c) dimers that both make topological sense with respect to membrane location and are formed largely by FNIIIc-mediated contacts. Both bury more than 1,000 Å^2 of surface area in the dimer interface, comparable to the 1,300 Å^2 buried when Ang1 binds to Tie2 (20). Both also involve residues that are evolutionarily well conserved, and neither interface would be impacted by Tie2 glycosylation. In dimer 1 (Fig. 2*B*) the C termini of the two copies of FNIIIc (linked to the Tie2 transmembrane domains) are separated by 50 Å, whereas this separation is 20 Å in dimer 2 (Fig. 2*C*).

The dimer 1 interface (Fig. 2*B*) primarily involves loops in the FNIIIb/FNIIIc boundary region, notably the FNIIIb/c linker, the FNIIIb EF loop, and the FNIIIc BC and FG loops. At the center of this interface, two highly conserved amino acids (R608 in the FNIIIb EF loop and Y665 in the FNIIIc BC loop), along with water molecules, contribute to a nearly twofold symmetric interface (Fig. 2*B*, *Right*). This central contact is augmented by several other (largely polar) interactions to bury 1,056 Å^2 (56% polar, 44% nonpolar), and for which the Pisa server estimates a

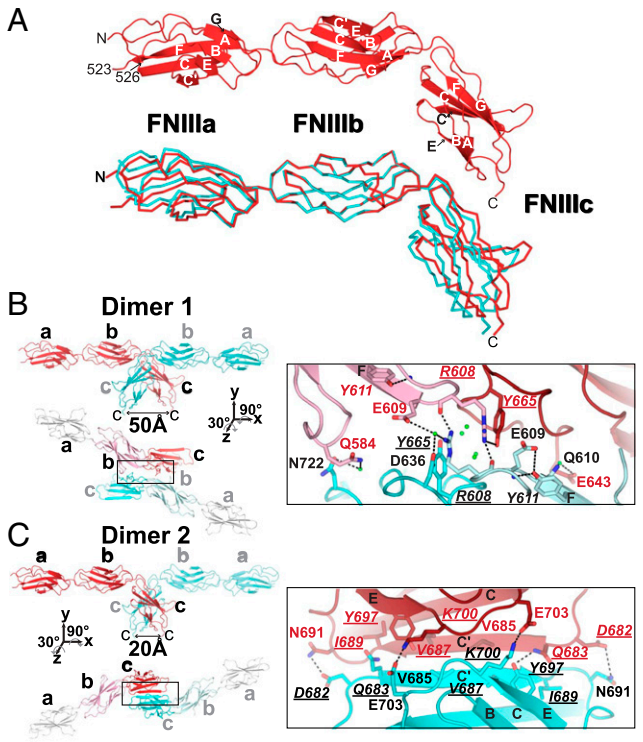

Fig. 2. Crystal structure of Tie2(FNIIIa–c) dimers. (*A*, *Upper*) Overall structure of Tie2(FNIIIa–c), with strands labeled using C2-set Ig domain nomenclature. (*Lower*) An overlay of the Cα trace for each of the two Tie2(FNIIIa–c) molecules in the asymmetric unit is shown (chain A is red; chain B teal), using FNIIIb Cα positions for alignment. (*B* and *C*) Cartoon views of each feasible Tie2(FNIIIa–c) dimer observed in the crystals. (*B*) Dimer 1. (*C*) Dimer 2. The red molecule is in the same orientation in *B* and *C*, and a detailed view of each dimer interface is shown in the box on the right. Water molecules are shown as green spheres, and predicted hydrogen bonds are shown as dashed lines. To improve contrast, in the views of the dimer interface, FNIIIc, FNIIIb, and FNIIIa are colored in progressively lighter shades of red (chain A) or teal (chain B). Residues mutated for cellular studies are underlined and italicized. Y611, found mutated in primary congenital glaucoma (23), is also italicized in *B*, and its interactions with the H606 backbone and E609 side chain are shown.

solvation free energy gain of −2.0 kcal/mol. Additional contributions to the interface are made by Q584 in the FNIIIb C/C′ loop (via water), E609 and Q610 (via water) in the FNIIIb EF loop, and D636 and E643 in the FNIIIb/c linker (Fig. 2*B*, *Right*). Importantly, the side-chain of Y611, depicted in Fig. 2*B*, appears to help position the EF loop by interacting with the H606 backbone amide and the E609 side chain (Fig. 2*B*, *Right*). A Y611C mutation was recently reported as a Tie2 loss-of-function mutation in primary congenital glaucoma (23) and was found to impair Ang1-induced Tie2 phosphorylation, further implicating the dimer 1 interface in Tie2 activation in vivo.

Dimer 2 (Fig. 2*C*) is mediated entirely by contacts between two FNIIIc domains, with antiparallel association of their C′ β-strands yielding an eight-stranded β-sheet across the two domains. Hydrophobic side chains of V685, V687, and I689 on strand C′, all of which would be exposed in a Tie2 monomer, are occluded from solvent as a result of this β-sheet extension (Fig. 2*C*, Right). This layer of the interface is completed by van der Waal's packing of side chains on the outer face of the C′ β-strand, together with flanking polar interactions involving D682, Q683, N691 (in β-strand C′), and Y697 (in β-strand E). A second layer of the dimer 2 interface is dominated by an intermolecular salt bridge between E703 and K700 in the EF loop (Fig. 2*C*, *Right*). Residues involved in these interactions are conserved or homologous as far as zebrafish, and the dimer 2 interface buries a total surface area of 1,382 Å^2 (53% polar, 47% apolar).

Mutational Analysis Implicates Dimer 1 in Ang1-Stimulated Tie2 Phosphorylation. To assess the biological relevance of the two FNIIIc-mediated dimers, we introduced mutations designed to disrupt them and analyzed the effect on Tie2 activation by Ang1. We used HEK-293 cells as a null background in which the molecular properties of Tie2 can be studied without confounding influences of other interacting proteins present in its normal contexts. Stably transfected HEK-293 cells expressing wild-type or mutated Tie2 proteins were sorted using flow cytometry to produce populations of transfected cells with matched, moderate cell-surface expression levels of Tie2 (also confirming proper receptor folding). Sorted cells were expanded, serum starved, and stimulated with antibody-clustered Ang1 as described (28). Levels of phosphorylated and total Tie2 were then determined by immunoblotting with anti-phosphotyrosine and anti-Tie2, respectively. To disrupt dimer 1, we mutated R608 and Y665 (Fig. 2*B*), both individually and in combination, to alanine. As shown in Fig. 3*A*, mutation of either residue (or both) essentially abolished Ang1-induced Tie2 phosphorylation. For R608A, no increase above background phosphorylation could be detected upon the addition of Ang1. When the Y665A mutation was included, basal phosphorylation was elevated, but no further increase was seen upon Ang1 stimulation (Fig. 3*A*). Total Tie2 expression for the R608A/Y665A mutant was significantly elevated, but cell-surface levels were not, suggesting intracellular accumulation of this doubly mutated variant and perhaps reflecting folding or trafficking defects. In parallel, we introduced the R608A or Y665A substitutions into sTie2 and found that both significantly disrupted sTie2 dimerization seen by SE-AUC (Fig. 3*B*), increasing K_d values by approximately eightfold (R608A) and 15-fold (Y665A) over wild type.

To disrupt dimer 2, two strategies were required because this interface primarily involves main-chain contacts that are difficult to disrupt with side-chain substitutions. In one set of mutations, we introduced a bulky, charged side-chain into the hydrophobic core of the dimer (V685R, V687R, or I689R). The V685R variant expressed poorly at the cell surface. V687R and I689R Tie2 variants both expressed well, but showed slightly increased (rather than impaired) Ang 1 sensitivity (Fig. 4*A*). In a second

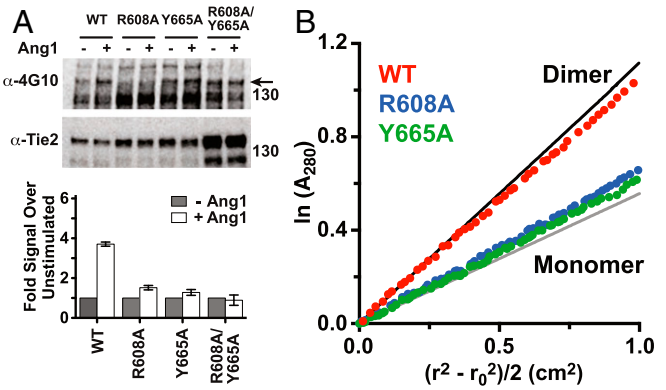

Fig. 3. Mutations in the dimer 1 interface impair Tie2 activation and dimerization. (*A*) Activation of wild-type or mutated Tie2 in HEK-293 cells with clustered Ang1 was assessed by immunoblotting with anti-phosphotyrosine (*Upper*) and anti-Tie2 (*Lower*). Normalized levels of Ang1-induced Tie2 phosphorylation were averaged over at least three experiments and are plotted (±SD). (*B*) The R608A and Y665A mutations were also introduced into sTie2, which then was analyzed by SE-AUC. Global fitting of data from multiple speeds and concentrations provided K_d estimates of ~15 μM and 25 μM for dimerization of the R608 and Y665 variants, respectively.

approach, we disrupted flanking and "second-layer" interactions in the dimer 2 interface by replacing charged (D682 and K700) or polar (Q683 and Y697) residues with alanine. All the variants shown in Fig. 4 also expressed well as soluble extracellular regions and formed dimers in solution, arguing against misfolding problems. Neither a D682A/Q683A double mutation nor a K700A mutation seemed to affect the response to Ang1 (Fig. 4*B*). The Y697A mutation, however, did reduce sensitivity to Ang1 (Fig. 4*B*). Although most dimer 2 interface mutations did not affect Tie2 activation, the Y697A data suggest that dimer 2 could play a role in Tie2 activation. Indeed, in the companion paper in this issue of PNAS (29), Leppänen et al. observe dimer 2 in two different crystal forms of a Tie2 FNIII domain fragment and provide further mutational evidence for its importance. Given the suggestions that higher-order oligomers are important in Tie2 signaling (14, 30), we hypothesize that both of the crystallographically observed interfaces may be important, as discussed below, although mutational analysis suggests that dimer 1 predominates in solution.

Small-Angle X-Ray Scattering Analysis of sTie2 Dimers. Because either mode of FNIII domain dimerization seen in our crystals suggests a surprisingly extended and "splayed out" conformation for sTie2 dimers, we were interested in determining whether sTie2 dimers have this characteristic in solution. We generated structural models of both potential sTie2 dimers by superimposing PDB entry 4K0V (which contains the LBR and FNIIIa of Tie2) onto each dimer structure by overlaying the shared FNIIIa Cα positions. The resulting model for dimer 1 is presented in Fig. 5*A* and shows the two LBRs splayed apart and separated by almost 300 Å. To determine whether this model is reasonable, we collected small-angle X-ray scattering (SAXS) data for sTie2 at three different protein concentrations (25, 38, and 50 μM, all >15-fold above K_d for dimerization). Scattering profiles were similar for each concentration analyzed, and forward scatter [$I(0)$] measurements using appropriate standards yielded an sTie2 molecular mass of 177.3 ± 8 kDa, corresponding to a dimer. Analysis of the SAXS data suggested a highly elongated dimer with maximal dimension (D_{max}) of ~300 Å and radius of gyration (R_g) of 105.4 ± 1.9 Å (Fig. 5*B*). We took

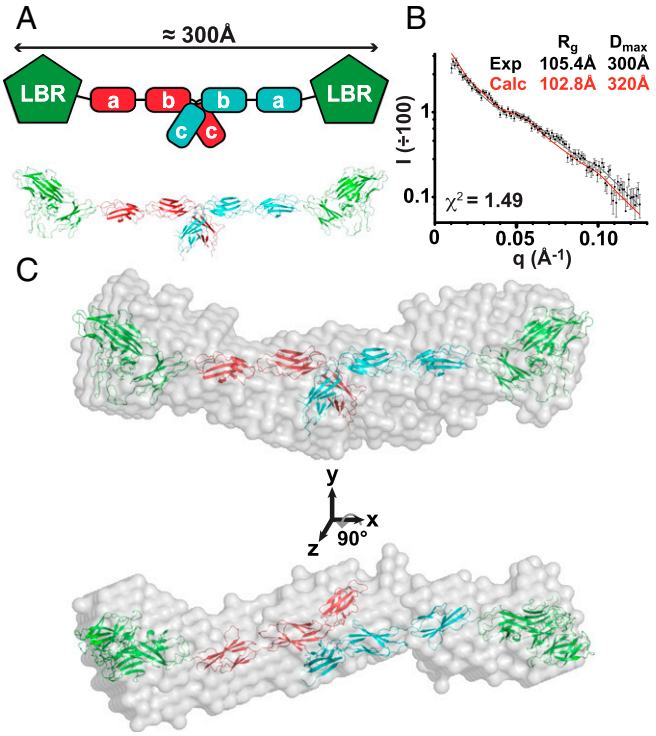

Fig. 5. SAXS analysis of sTie2 dimers. (*A*) Schematic and ribbon view of a complete sTie2 dimer model based on Tie2(FNIIIa–c) dimer 1, generated by superimposing PDB entry 4K0V (21) on dimer 1 from Fig. 2*B* guided by FNIIIa Cα positions. (*B*) The SAXS profile of sTie2 (black circles) shown as the recorded intensity as a function of the momentum transfer, *q*. Superimposed on the experimental data is the theoretical scattering profile for the model shown in *A* with $Man_9GlcNAc_2$ oligosaccharides modeled onto each of the nine glycosylation sites (red curve) or without modeled glycosylation (gray curve), calculated using CRYSOL (31), which gives a reasonable fit (χ^2 = 1.49 as defined by CRYSOL for glycosylated sTie2). Experimental and model (glycosylated) R_g and D_{max} values are listed in black and red text, respectively. (*C*) Two orthogonal views of the experimental SAXS-derived envelope for the sTie2 homodimer, shown in a gray transparent surface representation. The dimer 1-based sTie2 model was docked into the envelope in the same orientation as in *A* (and in Fig. 2*B*). Fig. S2 shows a similar analysis for dimer 2.

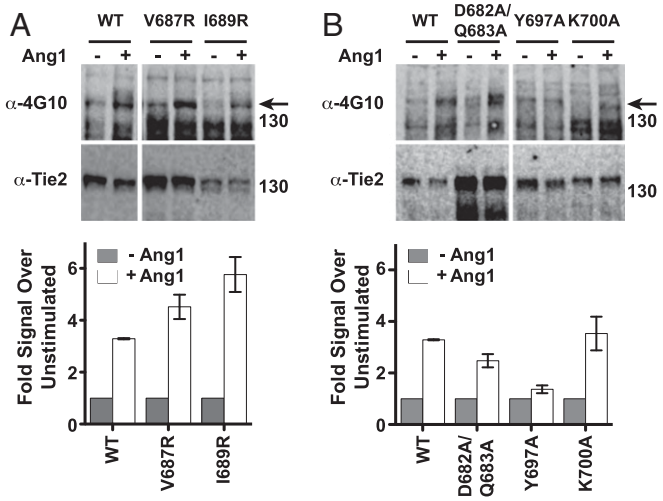

Fig. 4. Mutations in dimer 2 have less influence on Tie2 activation. Residues in the dimer 2 interface in β-strand C′ (*A*) or involved in polar interactions in the second layer (*B*) were mutated to alanines, and receptor activation with clustered Ang1 was assessed as in Fig. 3. In the lower panels, quantitation (mean ± SD) of normalized fold increase in Tie2 phosphorylation upon Ang1 stimulation is based on at least three repeats.

the sTie2 model shown in Fig. 5*A*, added glycans, and used CRYSOL (31) to generate a theoretical scattering profile (red line in Fig. 5*B*) that we superimposed on the experimental SAXS data (black points in Fig. 5*B*). The model gives a reasonable fit, with a SAXS fitting score (χ^2) as defined in CRYSOL (31) of 1.49. The model also has a calculated D_{max} of 320 Å and a R_g of 103 Å, in good agreement with experimental values. Interestingly, a similar analysis for dimer 2 gave essentially the same outcome, with a χ^2 SAXS fitting score of 1.36 and calculated D_{max} and R_g values of 325 Å and 108 Å, respectively (Fig. S2). Shape reconstruction from the scattering data, with no symmetry constraints or initial model, yielded extended low-resolution envelopes that could equally accommodate an sTie2 dimer based on either dimer 1 (Fig. 5*C*) or dimer 2 (Fig. S2), regardless of the presence of glycans, but could not accommodate higher-order oligomers [as confirmed by the $I(0)$ measurement]. These models are also consistent with lollipop-like Tie2 ECR structures seen by rotary shadowing electron microscopy (32). Although this earlier work did not assess dimerization per se, electron micrographs of sTie2–Fc fusion proteins showed the globular LBR extending out from a globular Fc dimer in a manner resembling our SAXS envelopes.

Model for Tie2 Clusters. The existence of two possible modes of FNIII domain-mediated sTie2 dimerization, together with evidence

for Tie2 clustering in cells (14, 30), suggests that both dimers might form simultaneously to yield higher-order receptor oligomers. Indeed, our mutational analysis allows the possibility that both dimer 1 and dimer 2 play roles in Ang1-induced Tie2 phosphorylation. A similar role for membrane-proximal FNIII domains in RTK clustering has been suggested in Eph receptor clustering, where multiple interfaces in the ECR of the receptor are required for localization and signaling (33, 34). To visualize possible FNIII domain-mediated clusters of the Tie2 ECR (Fig. 6*A*), we generated a hypothetical model of Tie2 ECR clustering driven by simultaneous formation of dimer 1 (A_1/B_1, A_2/B_2, and A_3/B_3 associations) and dimer 2 (B_1/A_2 and B_2/A_3 associations). Although the two bound Ang1 molecules in dimer 1 or dimer 2 are separated by more than 300 Å (Fig. 6*B*), only ∼53 Å separate Ang1 molecules bound to adjacent dimers in the cluster shown in Fig. 6. Given these dimensions, only highly clustered Ang1 molecules could engage both LBRs in a single Tie2 dimer simultaneously, but even an Ang1 dimer could effectively cross-link dimers to form the clusters shown in Fig. 6. These considerations suggest the intriguing possibility that Ang1 binding might "nucleate" the formation of the higher-order Tie2 oligomers suggested by our structural studies (which may or may not also include Tie1). This effect might be key for Tie2 signaling, with both dimerization interfaces described here contributing to ligand-induced receptor oligomerization and activation.

Discussion

Our finding that the soluble ECR of Tie2 dimerizes with a K_d value of ∼1.6 μM through its membrane-proximal region argues that full-length (unliganded) Tie2 may be significantly dimeric in cell membranes unless interactions with other species (such as Tie1) compete. By considering the mean distance between receptor molecules and translating this distance from two dimensions (in a membrane) to three, 10,000 Tie2 receptors per cell would correspond to an effective concentration of ∼1 μM. Orientational restriction will further enhance interactions between receptors in the membrane (27), and, by analogy with other RTKs, additional regions are likely to cooperate in driving Tie2 dimerization (13). Consistent with this suggestion, immunogold electron microscopy (35) and bimolecular fluorescence complementation (BiFC) assays (36) have argued that Tie2 forms ligand-independent dimers in the membranes of both endothelial cells and HEK-293 cells. Our crystal structure of FNIIIa–c suggests two possible modes of FNIII domain-mediated dimerization (Fig. 2), but our detection of only dimers (and not aggregates) in solution by SE-AUC and SAXS argues that only one of these modes dominates for sTie2 in solution. We cannot distinguish between the two different dimerization possibilities using SAXS (dimer 1 and dimer 2 give similar envelopes, as shown in Fig. 5 and Fig. S2). However, the fact that mutations in the dimer 1 interface (R698A and Y665A) yield sTie2 monomers in SE-AUC studies suggests that dimer 1 predominates in solution and also likely at the cell surface without ligand.

There is a substantial literature on the influence of Tie1 on Tie2 signaling (5, 15, 30, 37) and on direct interactions between the two receptors (12, 38), which might involve FNIII domain contacts of the sort described here. In particular, it is appealing to speculate that the backbone-mediated dimer 2 interactions could occur in both Tie2 homo-oligomers and Tie2/Tie1 hetero-oligomers. Indeed, Leppänen et al. (29) describe a model of Tie1/Tie2 heterodimerization through dimer 2-like interactions, which might allow Tie1 to modulate Tie2 clustering. Further comparison of the two studies suggests that the FNIII domains of Tie2 can engage in additional/alternative interaction modes. Although Leppänen et al. did not observe dimer 1 in their crystals (29), they saw an alternative mode of symmetric FNIIIb self-association that (as with our dimer 1) can occur alongside dimer 2-mediated interactions to cluster Tie2 (PDB ID codes 5MYA and 5MYB). This observation led them to propose a model for Tie2 clustering that closely resembles that shown in Fig. 6. Both models involve dimer 2 interactions, but use slightly different interfaces to link the resulting dimers into larger arrays: Dimer 1 largely engages the region between FNIIIb and FNIIIc, whereas the comparable interface identified by Leppänen et al. (29) is focused more squarely on FNIIIb. This intriguing interaction plasticity might allow distinct modes of receptor clustering in different cellular contexts or with different ligands (or ligand clusters) bound, possibly with altered signaling consequences.

Beyond potentially clustering Tie2 dimers as suggested in Fig. 6, simultaneous binding of two receptor-binding domains of an Ang oligomer to the Tie2 LBR also might induce conformational changes within the dimer if there is flexibility in the Tie2 ECRs. Yu et al. (21) argued that intimate interactions [burying 650 $Å^2$ between the third Ig domain of the LBR and FNIIIa in sTie2(ΔFNIIIbc)] render this interdomain linkage inflexible. The FNIIIb/c linkage in our structure buries ∼635 $Å^2$ (Table S2) and maintains precisely the same orientation in the structures reported by Leppänen et al. (29), indicating that it also is quite inflexible. By contrast, only ∼370 $Å^2$ are buried between FNIIIa and b, and these domains have quite different orientations in the different structures. The FNIIIa/b linkage therefore appears likely to be the primary site of flexibility in the Tie2 ECR, as further analyzed in Fig. S3 and Table S2.

Our structural analysis of the membrane-proximal FNIII domain-containing region of Tie2 simultaneously provides insight into how Angs might activate this receptor (and Tie1) and suggests avenues for therapeutic approaches for Tie receptor inhibition. That FNIIIc-mediated dimerization of Tie2's ECR is ligand-independent distinguishes it from most other RTKs. The suggestion that ligand binding may cluster these dimers to

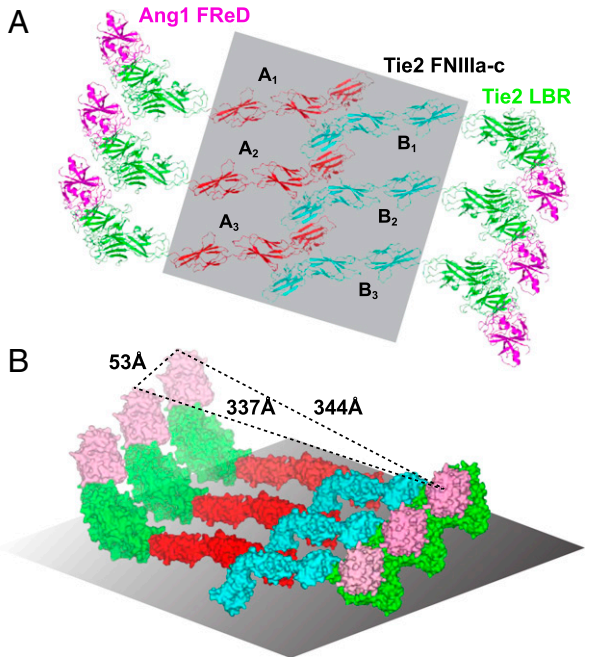

Fig. 6. Model for Tie2 homomeric clustering. A model showing how simultaneous use of both dimer 1 and dimer 2 interfaces could cluster the Tie2 ECR was generated by forming an array of Tie2(FNIIIa–c) based on crystal packing and superimposing PDB entry 4K0V (21) by FNIIIa domain overlay. (*A*) A ribbon representation with domains colored as in earlier figures and Ang1 in purple. The dimer 1 interface relates the A_1/B_1, A_2/B_2, and A_3/B_3 pairs. The dimer 2 interface relates the B_1/A_2 and B_2/A_3 pairs. (*B*) The same cluster shown in space-filling representation, with a view of how it might relate to the membrane surface (gray box).

activate the receptor, possibly in a manner influenced by Tie1, further distinguishes Tie2 from RTKs such as the insulin receptor (39) and *Caenorhabditis elegans* LET-23 (40), which have dimeric ECRs. The clustering model, together with the requirement for oligomeric ligands (14, 41), suggests similarities with the extended signaling arrays of Eph family receptors thought to be "seeded" by extracellular interactions (33, 34, 42). Indeed, like Tie1 and Tie2, the Eph family receptors have FNIII domains in their membrane-proximal regions that play important roles in clustering. It will be interesting to determine whether the analogous FNIII domains in the Tyro/Axl/Mer family (43) have similar self-association functions. The role played by FNIII domain-mediated interactions in the membrane-proximal region in Tie2 activation also makes them a potential Achilles' heel for the receptor. Inhibiting Tie receptor signaling has potential therapeutic value for the blockade of tumor angiogenesis (6), and targeting the FNIII domain-mediated interactions with antibodies might be an effective way of achieving this inhibition. Indeed, antibodies against Ig domains that make analogous interactions in the ligand-induced KIT (24) and VEGFR3 (25) dimers inhibit these receptors. The same approaches may be valuable for Tie2 and Tie1.

Materials and Methods

Protein Production and Crystallization. The entire human Tie2 ECR (residues 1–745: sTie2) and its variants were expressed by secretion from Sf9 cells. The FNIII domain-containing region (residues 443–745: Tie2(FNIIIa–c) was expressed in *E. coli*. Details are provided in *SI Materials and Methods*.

Crystallography and Biophysical Methods. Details of crystal structure determination, analytical ultracentrifugation, and SAXS are given in *SI Materials and Methods*.

Tie2 Activation Assays. Full-length Tie2 variants were stably expressed in HEK-293 cells, and activation by preclustered Ang1 (R&D Systems) was assessed by anti-phosphotyrosine immunoblotting as described in *SI Materials and Methods*.

ACKNOWLEDGMENTS. We thank the staff at the National Institute of General Medical Sciences (NIGMS) and National Cancer Institute (NCI) Structural Biology Facility at the Advanced Photon Source (GM/CA@APS) for help in data collection and members of the K.M.F., M.A.L., and Alitalo laboratories for valuable discussions. This work was supported in part by NIH Grants R01-GM099891 and R01-GM107435 (to M.A.L.) and R03-CA187021 (to K.M.F.). J.O.M. was the recipient of Postdoctoral Fellowship 123704-PF-13-034-01-DMC from the American Cancer Society. GM/CA@APS was funded by NCI Grant ACB-12002 and NIGMS Grant AGM-12006.

1. Partanen J, et al. (1992) A novel endothelial cell surface receptor tyrosine kinase with extracellular epidermal growth factor homology domains. *Mol Cell Biol* 12:1698–1707.
2. Davis S, et al. (1996) Isolation of angiopoietin-1, a ligand for the TIE2 receptor, by secretion-trap expression cloning. *Cell* 87:1161–1169.
3. Loughna S, Sato TN (2001) A combinatorial role of angiopoietin-1 and orphan receptor TIE1 pathways in establishing vascular polarity during angiogenesis. *Mol Cell* 7:233–239.
4. Augustin HG, Koh GY, Thurston G, Alitalo K (2009) Control of vascular morphogenesis and homeostasis through the angiopoietin-Tie system. *Nat Rev Mol Cell Biol* 10:165–177.
5. Jeltsch M, Leppänen VM, Saharinen P, Alitalo K (2013) Receptor tyrosine kinase-mediated angiogenesis. *Cold Spring Harb Perspect Biol* 5:a009183.
6. Huang H, Bhat A, Woodnutt G, Lappe R (2010) Targeting the ANGPT-TIE2 pathway in malignancy. *Nat Rev Cancer* 10:575–585.
7. Parikh SM (2016) Targeting Tie2 and the host vascular response in sepsis. *Sci Transl Med* 8:335fs9.
8. Suri C, et al. (1996) Requisite role of angiopoietin-1, a ligand for the TIE2 receptor, during embryonic angiogenesis. *Cell* 87:1171–1180.
9. Maisonpierre PC, et al. (1997) Angiopoietin-2, a natural antagonist for Tie2 that disrupts in vivo angiogenesis. *Science* 277:55–60.
10. Valenzuela DM, et al. (1999) Angiopoietins 3 and 4: Diverging gene counterparts in mice and humans. *Proc Natl Acad Sci USA* 96:1904–1909.
11. Brunckhorst MK, Wang H, Lu R, Yu Q (2010) Angiopoietin-4 promotes glioblastoma progression by enhancing tumor cell viability and angiogenesis. *Cancer Res* 70:7283–7293.
12. Seegar TC, et al. (2010) Tie1-Tie2 interactions mediate functional differences between angiopoietin ligands. *Mol Cell* 37:643–655.
13. Lemmon MA, Schlessinger J (2010) Cell signaling by receptor tyrosine kinases. *Cell* 141:1117–1134.
14. Davis S, et al. (2003) Angiopoietins have distinct modular domains essential for receptor binding, dimerization and superclustering. *Nat Struct Biol* 10:38–44.
15. Korhonen EA, et al. (2016) Tie1 controls angiopoietin function in vascular remodeling and inflammation. *J Clin Invest* 126:3495–3510.
16. Kim M, et al. (2016) Opposing actions of angiopoietin-2 on Tie2 signaling and FOXO1 activation. *J Clin Invest* 126:3511–3525.
17. Yuan HT, Khankin EV, Karumanchi SA, Parikh SM (2009) Angiopoietin 2 is a partial agonist/antagonist of Tie2 signaling in the endothelium. *Mol Cell Biol* 29:2011–2022.
18. Fukuhara S, et al. (2008) Differential function of Tie2 at cell-cell contacts and cell-substratum contacts regulated by angiopoietin-1. *Nat Cell Biol* 10:513–526.
19. Saharinen P, et al. (2008) Angiopoietins assemble distinct Tie2 signalling complexes in endothelial cell-cell and cell-matrix contacts. *Nat Cell Biol* 10:527–537.
20. Barton WA, et al. (2006) Crystal structures of the Tie2 receptor ectodomain and the angiopoietin-2-Tie2 complex. *Nat Struct Mol Biol* 13:524–532.
21. Yu X, et al. (2013) Structural basis for angiopoietin-1-mediated signaling initiation. *Proc Natl Acad Sci USA* 110:7205–7210.
22. Yuzawa S, et al. (2007) Structural basis for activation of the receptor tyrosine kinase KIT by stem cell factor. *Cell* 130:323–334.
23. Souma T, et al. (2016) Angiopoietin receptor TEK mutations underlie primary congenital glaucoma with variable expressivity. *J Clin Invest* 126:2575–2587.
24. Reshetnyak AV, et al. (2013) Structural basis for KIT receptor tyrosine kinase inhibition by antibodies targeting the D4 membrane-proximal region. *Proc Natl Acad Sci USA* 110:17832–17837.
25. Tvorogov D, et al. (2010) Effective suppression of vascular network formation by combination of antibodies blocking VEGFR ligand binding and receptor dimerization. *Cancer Cell* 18:630–640.
26. Barton WA, Tzvetkova D, Nikolov DB (2005) Structure of the angiopoietin-2 receptor binding domain and identification of surfaces involved in Tie2 recognition. *Structure* 13:825–832.
27. Grasberger B, Minton AP, DeLisi C, Metzger H (1986) Interaction between proteins localized in membranes. *Proc Natl Acad Sci USA* 83:6258–6262.
28. Bogdanovic E, Nguyen VP, Dumont DJ (2006) Activation of Tie2 by angiopoietin-1 and angiopoietin-2 results in their release and receptor internalization. *J Cell Sci* 119:3551–3560.
29. Leppänen V-M, Saharinen P, Alitalo K (2017) Structural basis of Tie2 activation and Tie2/Tie1 heterodimerization. *Proc Natl Acad Sci USA* 114:4376–4381.
30. Barton WA, Dalton AC, Seegar TC, Himanen JP, Nikolov DB (2014) Tie2 and Eph receptor tyrosine kinase activation and signaling. *Cold Spring Harb Perspect Biol* 6:a009142.
31. Svergun DI, Barberato C, Koch MHJ (1995) A program to evaluate X-ray solution scattering of biological macromolecules from atomic coordinates. *J Appl Cryst* 28: 768–773.
32. Macdonald PR, et al. (2006) Structure of the extracellular domain of Tie receptor tyrosine kinases and localization of the angiopoietin-binding epitope. *J Biol Chem* 281:28408–28414.
33. Seiradake E, Harlos K, Sutton G, Aricescu AR, Jones EY (2010) An extracellular steric seeding mechanism for Eph-ephrin signaling platform assembly. *Nat Struct Mol Biol* 17:398–402.
34. Xu K, et al. (2013) Insights into Eph receptor tyrosine kinase activation from crystal structures of the EphA4 ectodomain and its complex with ephrin-A5. *Proc Natl Acad Sci USA* 110:14634–14639.
35. Bogdanovic E, Coombs N, Dumont DJ (2009) Oligomerized Tie2 localizes to clathrin-coated pits in response to angiopoietin-1. *Histochem Cell Biol* 132:225–237.
36. Yamakawa D, et al. (2013) Ligand-independent Tie2 dimers mediate kinase activity stimulated by high dose angiopoietin-1. *J Biol Chem* 288:12469–12477.
37. Savant S, et al. (2015) The orphan receptor Tie1 controls angiogenesis and vascular remodeling by differentially regulating Tie2 in tip and stalk cells. *Cell Reports* 12:1761–1773.
38. Saharinen P, et al. (2005) Multiple angiopoietin recombinant proteins activate the Tie1 receptor tyrosine kinase and promote its interaction with Tie2. *J Cell Biol* 169:239–243.
39. Kavran JM, et al. (2014) How IGF-1 activates its receptor. *eLife* 3:e03772.
40. Freed DM, Alvarado D, Lemmon MA (2015) Ligand regulation of a constitutively dimeric EGF receptor. *Nat Commun* 6:7380.
41. Kim KT, et al. (2005) Oligomerization and multimerization are critical for angiopoietin-1 to bind and phosphorylate Tie2. *J Biol Chem* 280:20126–20131.
42. Seiradake E, et al. (2013) Structurally encoded intraclass differences in EphA clusters drive distinct cell responses. *Nat Struct Mol Biol* 20:958–964.
43. Lemke G (2013) Biology of the TAM receptors. *Cold Spring Harb Perspect Biol* 5:a009076.
44. Moore JO, Hendrickson WA (2009) Structural analysis of sensor domains from the TMAO-responsive histidine kinase receptor TorS. *Structure* 17:1195–1204.
45. Bork P, Downing AK, Kieffer B, Campbell ID (1996) Structure and distribution of modules in extracellular proteins. *Q Rev Biophys* 29:119–167.
46. Holm L, Rosenstrom P (2010) Dali server: conservation mapping in 3D. *Nucleic Acids Res* 38:W545–549.
47. Franke D, Svergun DI (2009) DAMMIF, a program for rapid ab-initio shape determination in small-angle scattering. *J Appl Cryst* 42:342–346.
48. Kozin M, Svergun D (2001) Automated matching of high- and low-resolution structural models. *J Appl Cryst* 34:33–41.
49. Aricescu AR, et al. (2007) Structure of a tyrosine phosphatase adhesive interaction reveals a spacer-clamp mechanism. *Science* 317:1217–1220.